Synchrotron X-ray Microtomography for 3D Imaging of Polymer Blends

ARTICLE *in* MACROMOLECULES · MARCH 2007

Impact Factor: 5.8 · DOI: 10.1021/ma062635+

Synchrotron X-ray Microtomography for 3D Imaging of Polymer Blends

Ahram Pyun,[†,§] Joel R. Bell,[‡,§] Kyu Hwang Won,[†] Byung Mook Weon,[†] Seung Kwon Seol,[†] Jung Ho Je,[*,†] and Christopher W. Macosko[*,‡]

X-ray Imaging Center, Department of Materials Science and Engineering, Pohang University of Science and Technology, Pohang 790-784, Korea, and Department of Chemical Engineering and Materials Science, University of Minnesota, Minneapolis, Minnesota 55455

Received November 16, 2006; Revised Manuscript Received January 17, 2007

ABSTRACT: Despite sufficient spatial resolution and routine operation, traditional electron microscopy (SEM and TEM) of polymer blend morphologies is limited to two dimensions (2D) and often requires tedious sample preparation. We have used a powerful X-ray imaging technique to visualize the morphology of polymer blends in three dimensions (3D). Images of polystyrene/high-density polyethylene (PS/HDPE) blend samples were constructed with microtomography using coherent synchrotron X-rays. Good contrast for blends with and without the PS phase removed (no other sample preparation was needed) was accomplished, and image quality is compared in the paper. High resolution (1 μm) images of relatively thick ($\sim$1 mm) blend samples were possible by adapting a sample stage equipped with high precision motor controls, by enhancing phase contrast through optimization of sample−scintillator distance, and by taking a large number of projection images (up to 1000) along different angles. Reconstructed slices were used to create 3D volume-rendered images of the blends. Coarsening of the cocontinuous morphology during annealing was monitored using extraction-free microtomography. Measurements of interfacial area per volume at varying annealing times agree with experimental results obtained using mercury porosimetry. It was also shown that SEM quantitative annealing results are limited at long annealing times due to the limitations of two-dimensional images of a three-dimensional morphology.

Introduction

The primary motivation for blending immiscible polymers is to create materials with combinations of properties superior to the components.[1] Blends with cocontinuous morphologies offer a variety of applications, including mechanical property enhancement,[2] electrically conductive blends,[3] moisture absorption,[4] and tissue scaffolds.[5] Cocontinuous morphologies are characterized by the mutual interpenetration of two phases and can form over a range of compositions, depending largely on the relative polymer viscosities, elasticity, interfacial tension, and mixing flow. Immiscible polymer blends are not thermodynamically stable;[6] therefore, postmixing processing such as molding or annealing can dramatically affect blend morphology.[7−10] Changes in morphology may reduce or eliminate benefits achieved by blending. It is important to understand and be able to control this phenomenon.

To fully understand blend properties, we must be able to visualize the morphology. A number of researchers have utilized two-dimensional (2D) techniques such as transmission electron microscopy (TEM) and scanning electron microscopy (SEM).[11,12] The images obtained by these techniques offer information on the 2D blend morphology, but the lack of three dimensions can cause misinterpretation of the true morphology. More recently, researchers have utilized electron tomography, laser scanning confocal microscopy (LSCM), and X-ray microtomography techniques to obtain three-dimensional (3D) images in the fields of materials science and medicine.[13−18] X-ray microtomography utilizes computerized tomography (CT), where many images of the same object are taken along different angles; suitable algorithms are then used to reconstruct different types of 2D and 3D images. Such a technique, know as "CAT scan" or "CT scan", has had a very important impact on medical diagnostics.

Table 1. Molecular Weight and Rheological Data at 170 °C for Blend Components

material	M_n (kg/mol)	M_w/M_n	η at 0.1 s^{-1} (Pa s)	η at 50 s^{-1} (Pa s)	η at 100 s^{-1} (Pa s)
PS	61	<1.1	3000	1800	1300
HDPE	18	5	3400	1300	1000

Sengupta et al. recently succeeded in the visualization of partially cocontinuous styrene(ethylene/butylene)styrene block copolymer (SEBS) phases in a SEBS/polypropylene (PP)/oil thermoplastic blend using electron tomography.[16] Samples needed to be stained, and then images of a thin slice (cryomicrotomed) were taken as the sample was rotated over 130°. After alignment of the slices, the data set was computed for 3D reconstruction. Verhoogt et al. were pioneers in using LSCM to visualize polymeric blends.[19] They imaged SEBS/poly(ether ester) blends and compared the results to SEM micrographs. Jinnai et al. also utilized LSCM to visualize cocontinuous blends, focusing on deuterated polybutadiene/polybutadiene (DPB/PB) blends.[17,20−22] The main limitation to this technique is that the depth of field is less than 50 μm. Montminy et al. and Pangerle et al. utilized a commercial X-ray CT system (1072 desktop microtomograph, SkyScan) to visualize polyurethane foams in 3D.[13,14] Elmoutaouakkil et al. used synchrotron X-ray microtomography to analyze the 3D structure of polymer foams.[23] This high X-ray flux enabled quantitative measurements of cell wall thicknesses. Ito et al. also utilized a commercial X-ray microtomography system (μCT20, Scanco Medical) to study trabecular bone parameters in 3D.[18] While the 3D parameters seemed to provide useful information for evaluating trabecular

* To whom correspondence should be addressed. E-mail: jhje@postech.ac.kr, macosko@umn.edu.
† Pohang University of Science and Technology.
‡ University of Minnesota.
§ These authors contributed equally to this work.

10.1021/ma062635+ CCC: $37.00
Published on Web 02/20/2007 PAGE EST: 6.8

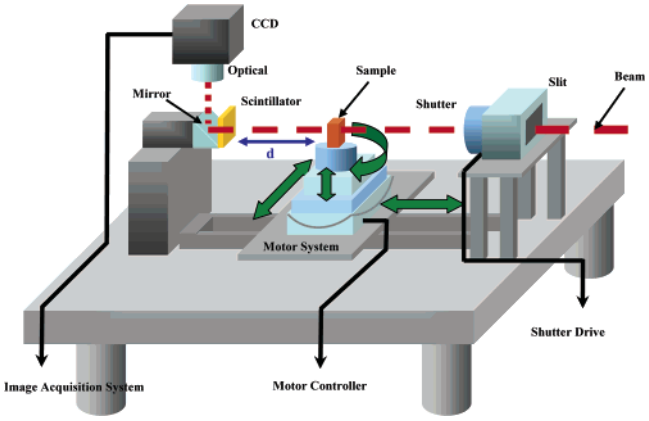

Figure 1. Schematic diagram of the synchrotron X-ray microtomography system. The sample to scintillator distance is *d*.

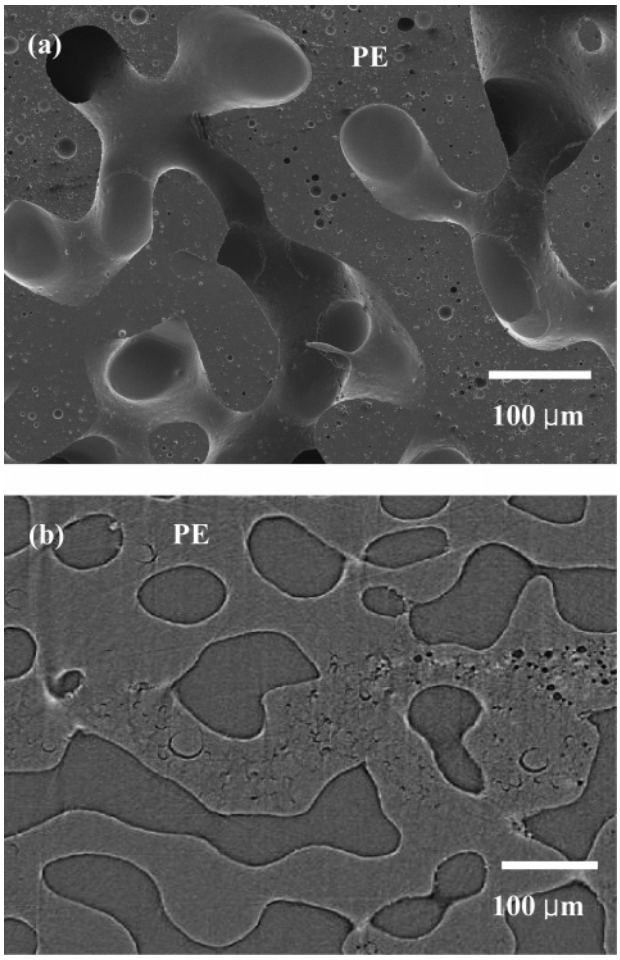

Figure 2. Images of (a) SEM micrograph and (b) reconstructed 2D slice from synchrotron X-ray microtomography for a 15 min annealed 50/50 PS/PE blend with PS extracted.

bone, further analysis of the results and better spatial resolution is needed. Weiss et al. obtained better spatial resolution in bone by using synchrotron X-ray microtomography.[24]

In this study, we compare synchrotron X-ray microtomography based on phase contrast imaging to SEM coupled with several image analysis techniques and mercury porosimetry (MIP). We used each method to image the coarsening of blend morphology in cocontinuous polystyrene/high density polyethylene (PS/HDPE) blends during annealing.

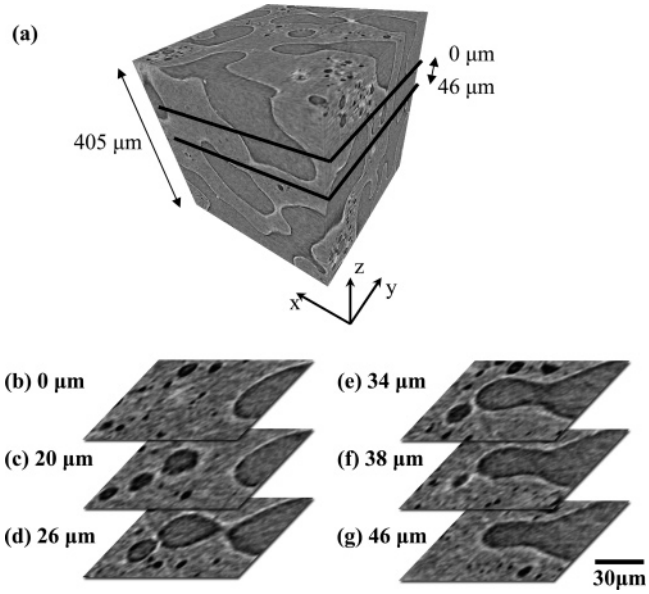

Figure 3. Reconstructed slices at different depths of a 15 min annealed 50/50 PS/PE blend with PS extracted. The PE phase is brighter. A volume-rendered cube (a) composed from reconstructed slices in three different planes (*xy*, *yz*, and *xz*). (b)−(g) are local areas of *xy* planes contained within a 46 μm vertical range: (b) reference depth of 0 μm, (c)−(g) increasing depth as indicated.

Experimental Section

Materials. Table 1 shows the properties of the blend components for these experiments. The system is identical to that used by Galloway et al.[25] The PS was anionically synthesized by Dow Chemical Co., and the HDPE is commercial Dow 4452N. Homopolymer viscosities were measured at 170 °C using a parallel plate rheometer (ARES, Rheometric Scientific Inc.).[25] At 170 °C, the polymers have closely matched viscosities.

Blend Preparation and Annealing. Blends were prepared by mixing the components in a Haake batch mixer (HBI System 90, Thermo Electron Co.) equipped with roller blades. Antioxidant (Irganox 1010, Ciba) was added at 0.2 wt % to the blends to reduce degradation. The blend composition was 50/50 PS/PE by weight. The materials were added in one step and mixed at 50 rpm (maximum shear rate = 48 s^{-1}) at a temperature of 170 °C for 10 min. The blends were then removed and quenched in liquid nitrogen within 1 min to freeze in the morphology.

Samples were annealed at 170 °C in a Wabash hydraulic press. Small blend chunks were placed between Teflon sheets in a 1 mm thick mold (2 mm for MIP) and then placed between two heated metal platens. The press was closed so that the sample thickness was restricted to 1 mm (2 mm for MIP), but no pressure was applied. Samples were annealed for time intervals of 2, 5, 10, 15, 30, 45, and 60 min. After annealing, cold water was flushed through the press platens to rapidly cool the samples (<100 °C) below the glass transition temperature of PS and melting temperature of PE; the cooling time (~1 min) was taken into consideration for annealing time determinations.

Microscopy and Image Analysis. Samples were cryo-microtomed at −120 °C, using a glass knife to generate clean and flat surfaces, and then visualized with scanning electron microscopy (SEM, JEOL 6500). Contrast between the phases was achieved by immersing each sample in toluene for 2 min to selectively remove the PS at the surface. The samples were then coated with 50 Å of platinum and imaged at 5 kV using SEM. Since the size scale of the domains and depth of field in the micrographs made it difficult to accurately detect the interface using automated methods, the phase boundaries were manually traced for this analysis. An analysis algorithm[26] was then used to determine the interface perimeter per unit area (*Q*) for each micrograph. For each annealing time, between 5 and 15 images were analyzed to determine the average *Q*.

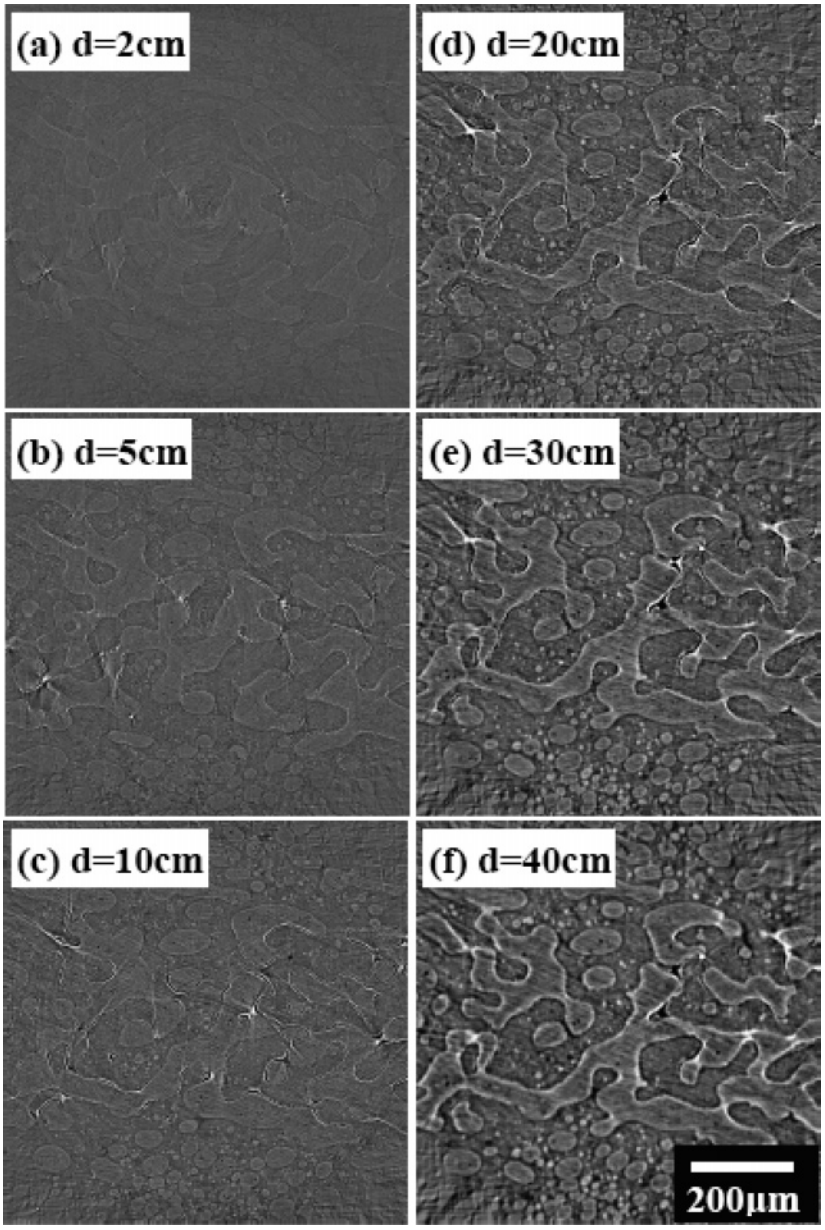

Figure 4. Reconstructed slices with different sample to scintillator distances, *d*: (a) 2, (b) 5, (c) 10, (d) 20, (e) 30, and (f) 40 cm for a 15 min annealed 50/50 PS/PE blend (unextracted). The brighter phase is PS.

Synchrotron X-ray Microtomography. Samples were cut from the 1 mm thick plaques, with a razor blade, into 2 mm × 2 mm squares. For experiments where one phase was selectively extracted, the samples were immersed in toluene for a day to entirely remove the PS phase and then dried in air. For experiments where no phases were extracted, no additional sample preparation was needed.

Experiments were performed on the ICPCIR (International Consortium of Phase Contrast Imaging and Radiology) 7B2 synchrotron X-ray microscopy high flux beamline at the Pohang Light Source (PLS). Figure 1 shows the experimental setup of the X-ray imaging system. In order to block and control the intensity of the X-ray beam, a mechanical shutter consisting of a Pt−Ir blade was used after the slit. The sample was mounted on a high precision motor-controlled stage with rotational, tilting, and translational resolutions of 0.002°, 0.0009°, and 250 nm, respectively. For background images, the sample is rotated 180° and is moved out of the path of the beam. After passing through the sample, the transmitted X-ray beam is converted by a scintillator to visible light, reflected by a silicon wafer, and then magnified by an optical lens. The scintillator is a polished $CdWO_4$ single crystal (30 × 30 × 0.3 mm^3, Nihon Kessho Koogaku Co., Ltd.) and generates visible light within the wavelength range of 470−540 nm. After magnification, the image is captured by a camera and image acquisition system.

Several images are averaged into one image at every 0.18° increment of rotation. This process is repeated 1000 times and takes about 1 h. The field of view is tunable by adapting different magnification lens and consists of 1600 × 1200 pixels. The image set was reconstructed by four parallel computers equipped with a reconstruction algorithm. Reconstructed slices consist of 1600 × 1600 pixels in the *x* and *y* dimensions. Vertically stacked 2D slices were constructed into volume-rendered 3D images using Amira software. Parameters such as interfacial area and volume were determined from these 3D images.

Mercury Intrusion Porosimetry. An additional technique used to measure pore diameter coarsening during annealing was mercury intrusion porosimetry (MIP). Yuan and Favis showed that MIP could be used to measure pore size in cocontinuous polymer blends as long as the samples were sufficiently thick (2 mm).[8] Samples with consistent weight, after extraction for 3 days with toluene (∼0.3 g), and thickness (2 mm) were measured at various annealing times using MIP (Micrometrics Poresizer 9320). The samples were placed

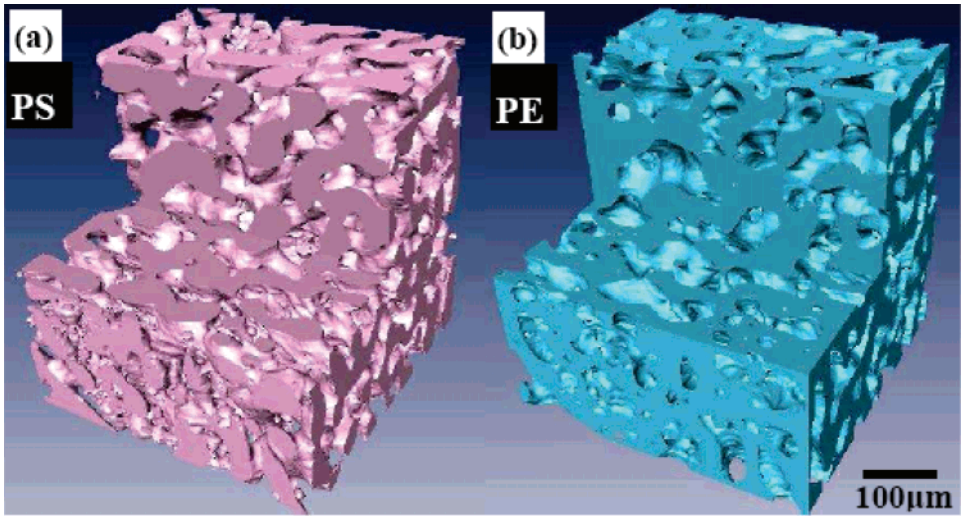

Figure 5. Volume-rendered images of (a) PS phase and (b) PE phase for a 15 min annealed 50/50 PS/PE blend (unextracted). (b) is the inverse of (a) and demonstrates that either phase can be used for calculations of surface area and pore diameter.

under vacuum in a 5 mL container, mercury was introduced into the container, and then the mercury was forced into the pores by applying incremental external pressure. The equipment calculates a volume average pore diameter and pore size distribution using the Washburn equation:[27]

$$Pr = -2\cos\theta$$

where P is the applied pressure and r is the pore radius. For mercury, the surface tension $\sigma = 485$ dyn/cm and the contact angle $\theta = 130°$. Further experimental and theoretical details are given elsewhere in the literature.[28−30]

Results and Discussion

Microtomography of PS/PE Blends with Extraction. After the PS is extracted with toluene and the sample is dried, the PS regions are filled with air. The PE phase has a much higher X-ray absorbency than air, and by adapting edge enhancement[31] induced by phase contrast, the contours of PE were imaged in the blend samples. An appropriate distance (∼20 cm) between the sample and scintillator was used to obtain optimal contrast (see Figure 1). A 2D reconstructed slice is shown in Figure 2b, from which phase dimensions can be determined. A SEM micrograph from another region of the same sample is shown in Figure 2a. There is good correlation between the two methods, with slight depth of field present in the SEM micrograph. Moreover, the cocontinuity of the PE phase can also be clearly observed in the vertically stacked reconstruction slice images in Figure 3. From these figures it can be seen that there is always a fraction of each phase that is trapped in drops, but this amount is less than 5% for our system. This was confirmed with solvent extraction, which is a technique often employed for studying extractables in cocontinuous polymer blends.[32]

Microtomography of PS/PE Blends without Extraction. Remarkable differentiation between the PS and PE phases was obtained using phase contrast. The interaction of electromagnetic radiation (X-rays) with matter depends on the complex refractive index of matter, $n = 1 - \delta + \beta i$.[15] The real part (δ) is associated with phase contrast, which is due to edge-enhancement effects based on diffraction, refraction, and interference, whereas the imaginary part (β) underlies absorption contrast. Different polymer regions have different refractive indices and thus produce different lateral displacements of a collimated X-ray beam (which is provided by synchrotron X-ray sources). The interference between transmitted and displaced beams that occurs near the boundary regions of the two polymers makes dark and bright fringes, resulting in edge enhancement.

One of the most important parameters in edge enhancement is the sample to scintillator distance, d. Figure 1 shows the schematic of this distance, d. The fringes' widths become too large at too large a distance, inducing edge-blurring effects, while the fringes' widths become too small to be detected by the detector at too small a distance.[31] Boundaries between PS and PE phases became visible at an appropriate d. The effect of d on reconstructed image quality for a 15 min annealed 50/50 PS/PE blend is shown in Figure 4. There were only very weak signals near the scintillator, $d = 2$ cm, and phase boundaries are difficult to discern. As d increased, edge enhancement developed and complex structures were seen in the projection images. At $d = 40$ cm, edge enhancement was so exaggerated that phase boundaries begin to blur. Although reconstructed slices were not as clear as in the extraction-aided experiment (Figure 2), it was possible to define each region of the components at the optimal value of $d = 20$ cm.

Figure 5 exhibits volume-rendered images of the PS and PE phases separately for a 15 min annealed 50/50 PS/PE blend. Cross sections in each component fit perfectly to each other. Volume fraction of the PE is slightly larger than that of the PS because of different polymer melt densities, but interfacial area is the same for both phases. 64×10^6 ($400 \times 400 \times 400$ pixels^3) total voxels and 400 reconstructed slices were used in calculations. Depending on the magnification lens used, the resolution varies between 1 μm per voxel and 2 μm per voxel. This is not the total field of view of the sample, but larger volumes have computational restrictions.

Annealing of PS/PE Blends. Using extraction-free microtomography, we studied the effect of annealing on blend morphology for 50/50 PS/PE blends. Reconstructed slices with different annealing times (t) are shown in Figure 6, and an increase in phase size is easily seen in the 2D slices. Furthermore, volume-rendered 3D solid models of the PE phase for each annealing time are shown in Figure 7. Image resolution was sufficient over the entire range of phase sizes investigated (3−85 μm). This technique is limited at dimensions much less than 1 μm because of the CCD camera that collects the images with an optical lens. It is interesting to note that the cocontinuous morphology is maintained, but phase size coarsens during annealing. The number of voxels and reconstructed slices for computation was the same as Figure 5.

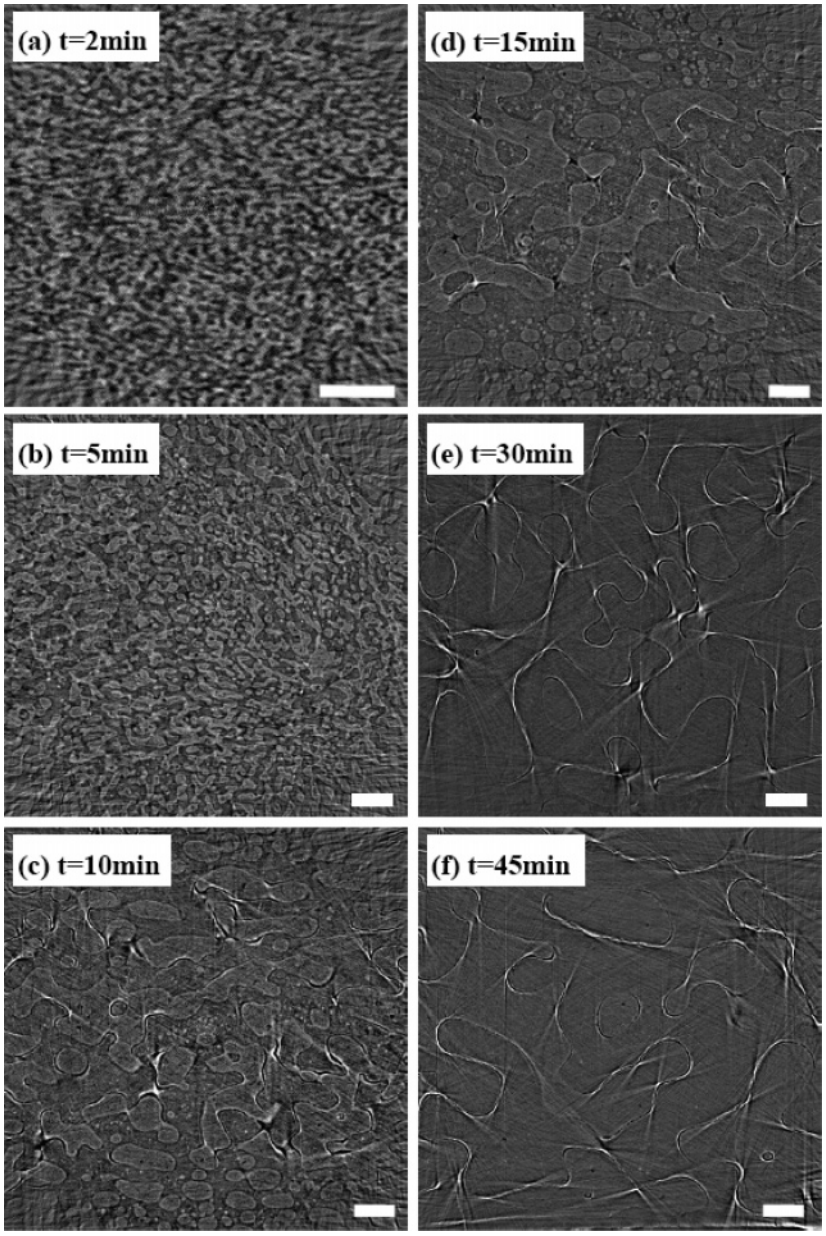

Figure 6. Reconstructed slices of (a) 2, (b) 5, (c) 10, (d) 15, (e) 30, and (f) 45 min annealed 50/50 PS/PE blends (unextracted). The brighter phase is PS. Scale bars = 100 μm.

The amount of interfacial area and volume of each phase was extracted from the 3D images. From this information, a value of interfacial area per volume (Q) can be calculated and monitored during annealing. We previously used 2D SEM images to estimate a Q value from measured perimeter per area values.[25,26] The inverse of Q gives an average pore size for the blends and is calculated for different annealing times. Figure 8 shows a plot of $1/Q$ vs annealing time measured for 50/50 PS/PE blends using 2D SEM images[25] and 3D volume-rendered microtomography images along with analogous pore size values vs annealing time measured by MIP.

The initial coarsening rates measured by all three techniques are in good agreement; however, the 2D measured values reach a plateau after ~20 min. The pore sizes measured by synchrotron X-ray microtomography and MIP continue to increase with increasing annealing time, but the slope does decrease after 20 min. A number of studies of coarsening in cocontinuous morphologies have reported a linear phase size increase (5−160 μm) during annealing.[8,10,33] Yuan and Favis[8] applied a method developed by Tomotika[34] and later adapted by McMaster[35] to model the coarsening growth rate as a linear function dependent on interfacial tension, zero-shear viscosity ratio, and capillary instabilities. While our results do show an initial linear coarsening rate, all three techniques indicate a second, slower coarsening rate at longer annealing times.

One possible explanation for this discrepancy is the loss of accuracy as the phase size approaches sample size. This is seen in the 2D SEM technique, where domain sizes approach the maximum field of view dimensions (500 × 600 μm, 0.3 mm^2, at 200× magnification), and the coarsening rate starts to plateau at ~50 μm. At magnifications lower than 200×, the edges of the sample (1 mm thick) hinder analysis. In addition, the 2D technique is limited by the assumption that perimeter per area is analogous to surface area per volume (Q) when sampling an area instead of a volume. The maximum field of view (800 × 800 μm, 0.64 mm^2) is larger for the 3D imaging technique, but only about twice as large. This is not significant, and thus the key difference is the third dimension in the maximum field of view (800 μm) and the fact that an actual value of Q is measured. Overall, the 2D technique is insufficient to fully

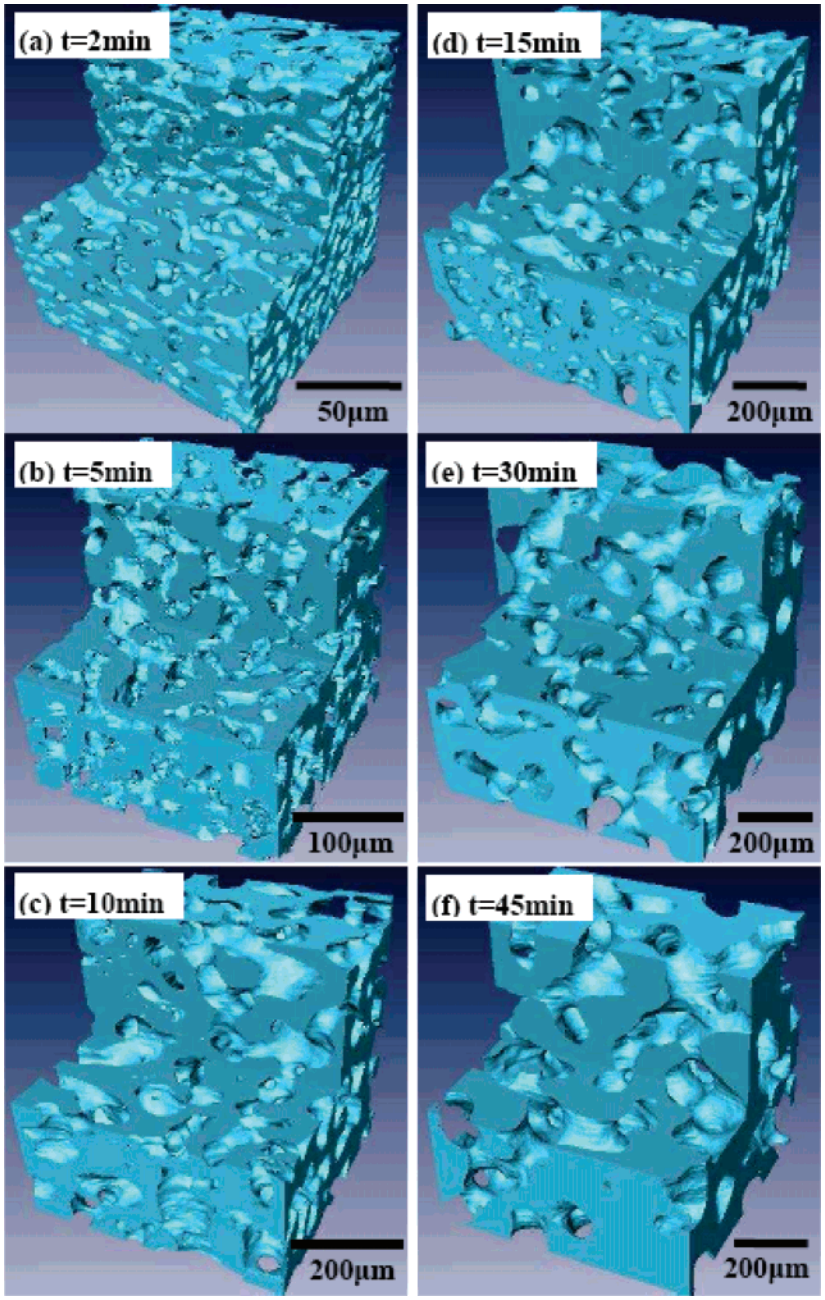

Figure 7. Volume-rendered images of (a) 2, (b) 5, (c) 10, (d) 15, (e) 30, and (f) 45 min annealed 50/50 PS/PE blends (unextracted). The PE phase is shown.

capture the morphology change and is not quantitatively accurate at large pore sizes.

MIP samples, on the other hand, are large (25 × 12.5 × 2 mm), and an actual pore size is calculated. Therefore, this test does not have the same limitations as the other techniques; however, no image of the morphology is obtained. The sample volume probed using MIP is ~500 mm^3; this is 2 orders of magnitude greater than the maximum volume probed using the 3D X-ray technique (0.5 mm^3), yet there is good agreement between their results at long annealing times. This further indicates the importance of a third dimension in the field of view for microscopy techniques. Results for MIP also show that the coarsening rate is not constant for our system and suggest that the phenomena of a slower coarsening rate at long annealing times is real.

Conclusions

Cocontinuous blends have been investigated because of their beneficial physical properties, which are directly attributed to their unique morphology. Thus, it is important to have techniques to measure cocontinuous morphology. Traditional microscopy techniques, such as SEM, give two-dimensional images and thus cannot be used to truly determine whether a blend's morphology is cocontinuous.

We have shown that coherent synchrotron X-ray microtomography is able to visualize the inner structures of low absorption materials such as polymer blends, with and without the extraction of one polymer phase. Extensive sample preparation was not needed, and depth of field for the samples was large (>500 μm). Remarkable visibility between PS and PE phases was established due to phase contrast. Using this technique, we were able to see the phase and connectivity of

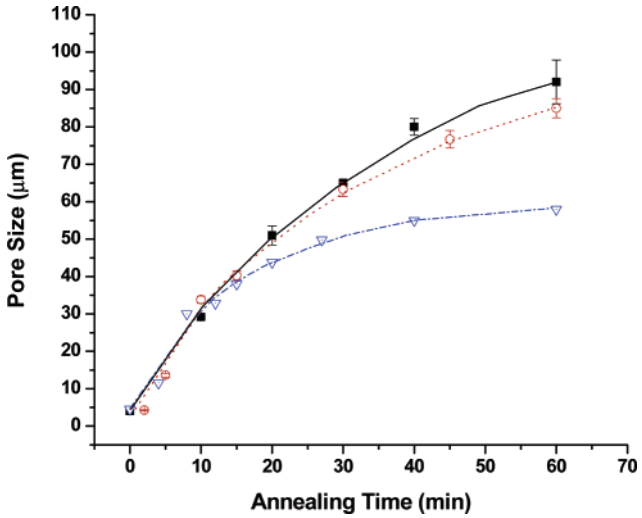

Figure 8. Plot of pore size vs annealing time of 50/50 PS/PE blends as measured with SEM[25] (▽), X-ray microtomography (○), and mercury porosimetry (■). Lines are to guide the eye and error bars are shown.

cocontinuous polymer blends in three dimensions and study its evolution during annealing. Quantitative information such as interfacial area and volume fraction for each phase was calculated and validated with mercury intrusion porosimetry (MIP). The results suggest that initial coarsening rates can be calculated using 2D SEM images; however, 2D imaging was limited at long annealing times. This is due to the morphology scale approaching the maximum field of view in our samples using SEM (0.3 mm^2), but more importantly because of the loss of accuracy when viewing 3D structures in 2D. MIP provides the most accurate measure of pore size during annealing, because of large sample volume (500 mm^3), but lacks the benefit of an image of the 3D structure.

We demonstrated that synchrotron X-ray microtomography is very a promising technique for morphological study of cocontinuous polymer blends. We expect that X-ray microtomography can be applied to diverse soft material systems to examine their internal structures and morphological information.

Acknowledgment. This work was supported by Creative Research Initiatives (Functional X-ray Imaging) of MOST/KOSEF, by the MRSEC Program of the National Science Foundation under Award DMR-0212302, by the National Science Foundation under Award DMS-0352143, and by a 3M Fellowship. Parts of this work were carried out in the Minnesota Characterization Facility which receives partial support from NSF through the NNIN program.

References and Notes

(1) Utracki, L. A. *Polym. Networks Blends* **1991**, *1*, 61.
(2) Xie, H.-Q.; Xu, J.; Zhou, S. *Polymer* **1991**, *32*, 95−102.
(3) RTP Company. *Conductive Thermoplastics*; RTP Company Technical Publication, 2005.
(4) Hekal, I. M. Desiccant entrained polymer: U.S. Patent No. 5,911,937, 1999.
(5) Washburn, N. R.; Simon, C. G., Jr.; Tona, A.; Elgendy, H. M.; Karim, A.; Amis, E. J. *J. Biomed. Mater. Res.* **2002**, *60*, 20−29.
(6) Paul, D. R.; Bucknall, C. B. In *Polymer Blends*; Paul, D. R., Bucknall, C. B., Eds.; John Wiley and Sons: New York, 2000; Vol. 1, pp 1−14.
(7) Yuan, Z.; Favis, B. *Biomaterials* **2004**, *25*, 2161.
(8) Yuan, Z.; Favis, B. *AIChE J.* **2005**, *51*, 271.
(9) Quintens, D.; Groeninckx, G.; Guest, M.; Aerts, L. *Polym. Eng. Sci.* **1990**, *30*, 1484−1490.
(10) Andradi, L. N.; Hellmann, G. P. *Polym. Eng. Sci.* **1995**, *35*, 693−702.
(11) Harrats, C.; Thomas, S.; Groeninckx, G. *Micro- and Nanostructured Multiphase Polymer Blend Systems: Phase Morphology and Interfaces*; Taylor & Francis: Boca Raton, FL, 2006.
(12) Potschke, P.; Paul, D. R. *J. Macromol. Sci.* **2003**, *C43*, 87.
(13) Pangerle, B. E.; Hammer, N. P.; Bidault, M. L.; Listemann, R. E.; Stevens, R. E.; Zhang, X. D.; Macosko, C. W. *Proc. Soc. Plast. Ind. Polyurethanes, Dallas, TX* **1998**, 247−253.
(14) Montminy, M.; Tannenbaum, A.; Macosko, C. *J. Colloid Interface Sci.* **2004**, *280*, 202−211.
(15) Margaritondo, G.; Hwu, Y.; Je, J. H. *Riv. Nuovo Cimento* **2004**, *27*, 1−40.
(16) Sengupta, P.; Noordermeer, J. *Macromol. Rapid Commun.* **2005**, *26*, 542.
(17) Jinnai, H.; Nishikawa, Y.; Koga, T.; Hashimoto, T. *Macromolecules* **1995**, *28*, 4782−4784.
(18) Ito, M.; Nakamura, T.; Matsumoto, T.; Tsurusaki, K.; Hayashi, K. *Bone* **1998**, *23*, 163.
(19) Verhoogt, H.; van Dam, J.; Posthuma de Boer, A.; Draaijer, A.; Houpt, P. M. *Polymer* **1993**, *34*, 1325−1329.
(20) Jinnai, H.; Nishikawa, Y.; Ito, M.; Smith, S. D.; Agard, D. A.; Spontak, R. J. *Adv. Mater.* **2002**, *14*, 1615−1618.
(21) Jinnai, H.; Nishikawa, Y.; Morimoto, H.; Koga, T.; Hashimoto, T. *Langmuir* **2000**, *16*, 4380−4393.
(22) Jinnai, H.; Yoshida, H.; Kimishima, K.; Funaki, Y.; Hirokawa, Y.; Ribbe, A. E.; Hashimoto, T. *Macromolecules* **2001**, *34*, 5186−5191.
(23) Elmoutaouakkil, A.; Fuchs, G.; Bergounhon, P.; Peres, R.; Peyrin, F. *J. Phys. D: Appl. Phys.* **2003**, *36*, A37.
(24) Weiss, P.; Obadia, L.; Magne, D.; Bourges, X.; Rau, C.; Weitkamp, T.; Khairoun, I.; Bouler, J.; Chappard, D.; Gauthier, O.; Daculsi, G. *Biomaterials* **2003**, *24*, 4591.
(25) Galloway, J. A.; Jeon, H.; Bell, J. R.; Macosko, C. W. *Polymer* **2005**, *46*, 183.
(26) Galloway, J. A.; Montminy, M. D.; Macosko, C. W. *Polymer* **2002**, *43*, 4715.
(27) Washburn, E. W. *Phys. Rev.* **1921**, *17*, 273.
(28) Good, R.; Mikhail, R. *Powder Technol.* **1981**, *29*, 53.
(29) Balker, A.; Relthaar, A. *Ind. Eng. Chem. Prod. Res. Dev.* **1982**, *21*, 590.
(30) Lowell, S.; Shields, J. E. *Powder Surface Area and Porosity*; Chapman & Hall, Ltd.: London, 1991.
(31) Hwu, Y.; Tsai, W.; Groso, A.; Margaritondo, G.; Je, J. *J. Phys. D: Appl. Phys.* **2002**, *35*, R105.
(32) Galloway, J. A.; Macosko, C. W. *Polym. Eng. Sci.* **2004**, *44*, 714−727.
(33) Veenstra, H.; van Dam, J.; Posthuma, de Boer, A. *Polymer* **2000**, *41*, 3037−3045.
(34) Tomotika, S. *Proc. R. Soc. London, Ser. A* **1935**, *A150*, 322.
(35) McMaster, L. P. *Adv. Chem. Ser.* **1975**, *142*, 43.

MA062635+